Insights into the tussock growth form with model data fusion

Salvatore R. Curasi*[,1,3, https://orcid.org/0000-0002-4534-3344], Ned Fetcher[2, https://orcid.org/0000-0003-2604-299X], Kelseyann S. Wright[1], Daniel P. Weldon[1], Adrian V. Rocha[1, https://orcid.org/0000-0002-4618-2407]

[1]Department of Biology, University of Notre Dame, Notre Dame, IN 46556, USA; [2]Institute for Environmental Science and Sustainability, Wilkes University, Wilkes-Barre, PA 18766, USA; *Correspondence: Salvatore R. Curasi, e-mail: scurasi@nd.edu, tel: +1-574-631-2874, fax: +1-574-631-7413; [3]Current affiliations: Department of Geography and Environmental Studies, Carleton University, Ottawa, Ontario K1S 5B6, Climate Research Division, Environment and Climate Change Canada, Victoria, BC, V8W 2Y2, Canada.

Keywords: Arctic, climate change, climate change, *Eriophorum vaginatum*, model-data fusion, tundra, tussock

Article type: Full paper

Summary

Some rhizomatous grass and sedge species form tussocks that impact ecosystem structure and function. Despite their importance, tussock development and size controls are poorly understood due to the decadal to centennial timescales over which tussocks form.

We explored mechanisms regulating tussock development and size in a ubiquitous arctic tussock sedge (*Eriophorum vaginatum*) using field observations and a mass balance model coupled to a tiller population model. Model data fusion was used to quantify parameter and prediction uncertainty, determine model sensitivity, and test hypotheses on the factors regulating tussock size.

The model accurately captured the dynamics of tussock development, characteristics, and size observed in the field. Tussock growth approached maximal size within several decades, which was determined by feedbacks between the mass balance of tussock root necromass and density-dependent propagation of new tillers. The model also predicted that tussock maximal size was primarily regulated by tiller root productivity and necromass bulk density, and less so by tiller demography. These predictions were corroborated by field observations of tussock biomass and root characteristics.

The study highlights the importance of belowground processes in regulating tussock development and size and enhances our understanding of the influence of tussocks on arctic ecosystem structure and function.

1. Introduction

Rhizomatous grass and sedge species often form clumps of individual tillers that result in the formation of tussocks (Oliva et al., 2005, Lawrence and Zedler, 2011, Derner et al., 2012, Wein, 1973). Tussock-forming species are often considered ecosystem engineers or foundation species and influence a variety of ecosystem properties including micro-topography, soil moisture, soil carbon (C) accumulation, and species diversity (Peach and Zedler, 2006, Varty and Zedler, 2008, Benscoter and Vitt, 2008, Elumeeva et al., 2017, Crain and Bertness, 2005, Qiao et al., 2020, Balke et al., 2012, Eldridge et al., 2010). This is especially true in the Arctic, where tussock cottongrass (*Eriophorum vaginatum*) forms elevated mounds of root necromass as a strategy to escape the poor growing conditions of waterlogged anoxic soils (Figure 1) (Lawrence and Zedler, 2011, Crain and Bertness, 2005, Chapin et al., 1979). Tussocks enhance arctic soil organic C stocks and have exhibited declines in abundance in some areas in response to recent climate change (McGraw et al., 2015, Box et al., 2019, Hobbie et al., 2017, Curasi et al., 2022, Macander et al., 2022). These declines are concerning since climate change has the potential to alter tussock formation, size, and abundance resulting in large regional losses and gains in arctic C stocks (Curasi et al., 2022).

Much of our understanding of cottongrass tussock formation is based on qualitative observations and demographic models that exclude the necromass that provides the structure on which tillers reside (Fetcher and Shaver, 1982, Fetcher and Shaver, 1983, Mark et al., 1985, Shaver et al., 1986a, Bennington et al., 2012b, McGraw et al., 2015). The exclusion of the links between necromass, tiller demography, and tussock C storage potential limits our ability to predict climate change impacts on tussocks (Curasi et al., 2019, Curasi et al., 2022, Bennington et al.,

2012a, McGraw et al., 2015). Tussocks are formed by a population of interconnected asexually propagating tillers that reside on an elevated surface created by the accumulation of root necromass and litter (Chapin et al., 1979, Wein, 1973, Mark et al., 1985). Tussocks have both above and below-ground components with their total mass being related to their diameter through allometric constraints on size and growth (Curasi et al., 2022, Chapin et al., 1979). The diameter of cottongrass tussocks rarely exceeds 50 cm, which suggests that there are limits to their maximum size and C storage potential (Fetcher and Shaver, 1982, Fetcher, 1983, Mark et al., 1985). Tussocks develop over decades to centuries with estimated ages for mature tussocks between 122 and 187 years based on tiller growth and turnover (Chapin et al., 1979, Wein, 1973, Mark et al., 1985). Tussock's long lifespan (i.e. decades to centuries) challenges our ability to understand the mechanisms that regulate their formation and size (Lawrence and Zedler, 2011, Mark et al., 1985, Fetcher and Shaver, 1982, Lawrence and Zedler, 2013, Oliva et al., 2005). This is unfortunate given their prominent role as a foundation species in the Arctic and hence their importance in predicting the ecosystem's response to climate change.

We hypothesize that tussock formation and size are controlled by three main types of factors: physical, structural, and demographic. Physical factors directly contribute to tussock C storage and include root production that increases tussock size as well as the decomposition of root necromass and dead tillers that reduces tussock size (Chapin et al., 1979, Curasi et al., 2022). In the Arctic, *Eriophorum vaginatum* has a deciduous root system that dies back at the end of each growing season and regenerates the following spring, thereby producing considerable necromass (Chapin et al., 1979, Ma et al., 2022). Structural factors directly relate to a tussock's structural composition and include the root necromass bulk density and the size of the tillers that reside

atop the tussock. Necromass comprises a majority (~70%) of total tussock mass, and its bulk density (g cm^{-3}) determines the amount of root necromass required to "build" a tussock of a given volume (Curasi et al., 2022). Tiller size is a structural factor that determines the maximal density of tillers that reside atop a tussock (Fetcher and Shaver, 1982). Demographic factors are associated with the initial per-capita birth rate, initial per-capita death rate, and per-capita population growth rate of the living tillers that reside atop the tussock (Bennington et al., 2012b, McGraw et al., 2015, Fetcher and Shaver, 1983). Here, we present a parsimonious tiller population model coupled with a mass balance model and determine the relative importance of these factors in determining tussock size and tussock C stocks. The model predictions were constrained with field measurements of tussock allometry, tiller characteristics, and tiller demography through model-data fusion using a Monte Carlo algorithm to predict model parameters.

2. Methods

2.1 Philosophy of approach

Parsimonious mathematical models are widely used for prediction and hypothesis testing in ecology and evolutionary biology, especially for long-term processes that are difficult to measure (Rastetter, 2017, Kyker-Snowman et al., 2022, Dietze et al., 2013). The strength of a parsimonious model is its tractability, while its weakness lies in its inability to represent every process, which may decrease a model's predictive value (Rastetter, 2017). Parsimonious model validation is often performed through comparison with observations, however, these comparisons do not account for the impacts of observation parameter uncertainty on model predictions. Recently, statistical techniques have been developed to constrain model predictions

and determine prediction uncertainty through the use of model-data fusion (Zobitz et al., 2011, Keenan et al., 2011). Model data fusion using a Monte Carlo algorithm statistically constrains model parameters so that model predictions closely match observations provided their uncertainty (Keenan et al., 2011, Keenan et al., 2012b, Wright and Rocha, 2018, Peng et al., 2011). Because model data fusion is iterative, it also can determine a model's sensitivity to parameter changes, providing insight into the importance of various model processes in making predictions (Wright and Rocha, 2018, Peng et al., 2011, Zobitz et al., 2011). Here we use model data fusion alongside a newly developed parsimonious model of tussock formation to determine the relative importance of physical, structural, and demographic factors in determining tussock size and tussock C stocks.

2.2 Temporal and spatial variability of in situ tussock size

We measured the spatial and temporal variability in tussock size to assess size controls and temporal changes (Figure S1). To quantify spatial variability, we measured the diameter and height above the moss surface of 2,321 tussocks across 46 sites along a latitudinal gradient across the North Slope of Alaska. Tussocks were selected for measurement if their centers intercepted a 200 m transect tape at each site. For each tussock, two perpendicular measurements of diameter were taken using tree calipers, and four measurements of height above the moss surface were taken with a ruler in each cardinal direction. To quantify the temporal change in site average tussock size, we repeated tussock diameter measurements at four sites that were surveyed in the late 1970s in 2016/2018 (Fetcher and Shaver, 1982). One site (Eagle creek bladed, EC-B) was cleared by a bulldozer in 1977 and represented a disturbed site with young developing tussocks. The other three sites (Eagle creek undisturbed EC-U, and Cape Thompson 1/2) were undisturbed and represented mature tussocks. Tussock diameters were averaged per

site and period and related to climate and height using linear regression. Climate data were obtained from WorldClim 2 and extracted using each site's GPS coordinates (Fick and Hijmans, 2017).

2.3 Tussock allometry, tiller characteristics, and decomposition

Tussocks were harvested during the peak of the growing season in 2016 at the Toolik Lake LTER site (n = 35) to quantify tussock allometry, tiller characteristics, and decomposition. For tussock allometry, we measured tussock mass, diameter, height above moss surface, and total above and belowground height. Tussock mass was separated into tiller leaf litter, brown/black root necromass, green living tillers, and white live roots. Bulk density was quantified from the dry weight of root necromass within a cylindrical core of known volume (5.7 cm diameter and ~30 cm long) taken through the center of each tussock. For tillers, we measured the number of living and dead tillers, annual tiller root production, living and dead tiller diameter, and tiller propagation rates for each harvested tussock. Tiller propagation was estimated as the number of newly developed secondary tillers without developed leaves divided by the number of living adult tillers. Tussocks were measured by taking two perpendicular measurements using tree calipers for diameters and four measurements using rulers for lengths. Tillers were measured by taking a single measurement at their base using calipers. All mass measurements were taken after oven drying the material at 60 °C for 48 hours. Samples of tussock root necromass (n = 76) and dead tillers (n =15) were set aside for a decomposition experiment using the mesh-bag technique (Karberg et al., 2008). For each sample, ~5 g of dry material was weighed, sealed in a mesh bag, and reweighed after a year in the field. The annual mass change in each mesh bag was used to

estimate negative exponential decay constants using methods described in Parker et al. (2018) and Andren and Paustian (1987).

2.4 Tussock Size Model

We developed a model for individual tussocks using a series of coupled differential equations describing tiller population dynamics and tussock mass balance (Figure 2). The model represented an individual tussock as a root necromass island that supported a population of living and dead tillers. The tussock island changed volume (V; cm^3) according to modeled changes in root necromass (ΔM: $g\ y^{-1}$) and average root necromass bulk density (ρ; $g\ cm^{-3}$) (Equation 1).

$$\frac{dV}{dt} = \frac{\Delta M}{\rho} \qquad \textbf{Equation 1}$$

Representing the tussock as a volume allowed for the relationship between tussock height and tussock radius to be defined using a 3-dimensional shape. We used the necromass bulk density, tussock radius, and tussock necromass measurements described in section 2.3 to fit an allometric relationship (i.e. tussock radius vs. necromass) using four common three-dimensional shapes: inverted cone, half-sphere, cylinder, and modified cylinder. The tussock shape was determined before model parameterization to avoid parameter identifiability and equifinality issues during model-data fusion (Beven, 2006, Keenan et al., 2011, Peng et al., 2011). Out of the four commonly used three-dimensional shapes, the modified cylinder minimized the mean absolute error between modeled and measured allometry (Figure S2a). The representation of a tussock as a modified cylinder indicates that changes in tussock radius are accompanied by linear changes in height. This was supported by measurements that demonstrated strong linear correlations between tussock radius and height above the moss surface ($y = 0.004 \pm 0.05 + 1.03x \pm 0.02$, $P <$

0.001, $R^2 = 0.55$), and tussock radius and total tussock height ($y = 9.09 \pm 1.5 + 1.52x \pm 0.16$, $P < 0.001$, $R^2 = 0.73$) (Figures S2b). Given this geometry, tussock radius at time t ($r(t)$; cm) was related to M at time t, ρ, and the fitted ratio between tussock height and radius (1.6) with equation 2.

$$r(t) = \sqrt[3]{\frac{M(t)}{1.6\pi\rho}} \qquad \textbf{Equation 2}$$

A tussock supports a total population (N_T; #) of living (N_A; #) and dead (N_D; #) tillers that occupy the top of the tussock (Equation 3).

$$N_T = N_A + N_D \qquad \textbf{Equation 3}$$

The change in the population of N_A was represented with a logistic growth model using an initial per-capita growth rate (r_A; y^{-1}) and a carrying capacity for live tillers (K_A; #) (Equation 4).

$$\frac{dN_A}{dt} = r_A N_A \left(1 - \frac{N_A}{K_A}\right) \qquad \textbf{Equation 4}$$

This representation of the living tiller population dynamics implements density-dependent reproduction rates, which is supported by observed declines in tiller reproduction rates as tussocks mature (Fetcher and Shaver, 1982, Fetcher and Shaver, 1983, Fetcher, 1983). Density-dependent reproduction is common in rhizomatous grasses as it reduces intraspecific competition and tiller overproduction (Antonovics and Levin, 1980, de Kroon and Kwant, 1991, de Kroon, 1993, Lonsdale and Watkinson, 1983, Fetcher, 1985, Barkham and Hance, 1982). Tiller mortality was modeled as being density independent because density-dependent mortality has

been shown to be nonexistent or weak in rhizomatous plants (de Kroon and Kwant, 1991, de Kroon, 1993). K_A was determined by the space atop the tussock for new tillers that was unoccupied by living and dead tillers. The total number of tillers that a tussock can support at time t ($\eta(t)$; #) was determined with a hexagonal packing model where tillers of an average diameter (θ; cm) optimally fill a circular area defined by the tussock radius at time t (Equation 5).

$$\eta(t) = \frac{\pi r(t)^2}{\theta^2\sqrt{12}} \qquad \textbf{Equation 5}$$

Hexagonal packing is common in clonal plants and organismal structures (i.e. honeycombs) and serves as a way to maximize packing density in a given area (Stephenson, 2003, Wolfram, 2002, Nazzi, 2016, Darwin, 1859, Bell, 1979, Oborny et al., 2012). Hexagonal packing on a circular area (Equation 5) was able to capture the total tiller population in harvested tussocks described in section 2.3 with a mean average percent error (MAPE) of 17% (Figure S3). This low MAPE validates the use of hexagonal packing in the model. To demonstrate the role of tiller packing on tussock development, we derived the packing index as the ratio between η and N_T (N_T/η). A packing index between 0 and 1 indicates a tussock with available carrying capacity, whereas a packing index of 1 indicates a completely packed tussock. K_A was calculated using equation 6.

$$K_A(t) = \eta(t) - N_D(t) \qquad \textbf{Equation 6}$$

The change in the population of N_D was a function of gains from the death of live tillers (d_A*N_A; # y^{-1}), and losses from the decomposition and removal of dead tillers atop the tussock (k_D*N_D; #

y^{-1}) (Equation 7). d_A (y^{-1}) was the initial per-capita death rate for live tillers that contributed to the dead tiller population, and k_D (y^{-1}) was the dead tiller decomposition and removal rate for dead tillers that made space for new tillers to form atop the tussock.

$$\frac{dN_D}{dt} = \overbrace{d_A N_A}^{Gains} - \overbrace{k_D N_D}^{Losses} \quad \textbf{Equation 7}$$

The mass balance of M was a function of the root necromass added to the tussock by live tillers ($\alpha * N_A$; g y^{-1}), and root necromass losses via decomposition ($k_M * M$; g y^{-1}) (Equation 8). α was the root input rate per tiller (g $tiller^{-1}$ y^{-1}) that adds mass and volume to the tussock, and k_M was the decomposition rate of root necromass (y^{-1}) that removed mass and volume from the tussock.

$$\frac{dM}{dt} = \overbrace{\alpha N_A}^{Gains} - \overbrace{k_M M}^{Losses} \quad \textbf{Equation 8}$$

The model had seven parameters that determined tussock development and size (Table 1). Physical factors were associated with α, k_M, and K_D, structural factors were associated with θ and ρ, and demographic factors were associated with r_A, and d_A. We used fitted parameters to calculate the per-capita birth rate using Equation 9 which was derived through algebraic manipulation of equation 4 when population growth is at steady state (methods S1; Figure S4).

$$b = d_A + r_A\left(1 - \frac{N_A}{K_A}\right) \quad \textbf{Equation 9}$$

Given the strong coupling between tussock mass balance, volume, and available space for tillers, we hypothesized that physical factors would primarily determine tussock size. The tussock size

model was solved numerically in R using the Runge-Kutta fourth-order method in the "deSolve" package (Soetaert et al., 2010, R Core Team, 2019), and parameterized using the model data fusion routine described in the next section (2.5).

2.5 Model parameterization with model-data fusion

Our tussock model was parameterized using a weighted least-squares two-step model-data fusion based on Keenan et al. (2012a), Richardson et al. (2010), and Wright and Rocha (2018). The uniform prior distributions for ρ, θ, α, and k_M were based on the maximum and minimum values observed in the field (Table 1). Relatively few samples of dead tiller decomposition were available in the field data, however, the available samples fell within the same range as the root necromass decomposition rates. Therefore, the uniform bounds for k_M were used for k_D as well. The bounds for r_A and d_A were determined based on detailed tiller demography measurements of cottongrass from Fetcher and Shaver (1983).

The model parameterization utilized three observational data streams: tussock radius surveyed across the North Slope, the relationship between tussock radius and tussock mass from our harvest of tussocks, and the ratio between the number of live tillers and tussock radius from our harvests. For each data stream, we calculated an individual cost function (j_i) as the total uncertainty-weighted squared data-model disagreement for each data type (equation 10) which is a function of the number of observations (N_i) for each data type (i), the data (y_i), and the value predicted by the model (p_i) (Richardson et al., 2010). The standard deviation of all the measurements was used as the uncertainty (δ_i) in the tussock radius and live tillers to radius ratio data streams. For the relationship between tussock radius and tussock mass, the uncertainty term

was based on the standard deviation of the paired tussock radius measurements (Richardson et al., 2012). Tussocks reach maturity within 250 years (Mark et al., 1985) and hence we incorporated an additional constraint (Richardson et al., 2010) wherein simulations were rejected if the tussock radius did not reach an asymptotic growth trajectory within that time.

$$j_i = \sum_{1}^{N_i} \left(\frac{y_i - p_i}{\delta_i} \right)^2$$ **Equation 10**

In step one, parameters were proposed using a normal distribution with a mean equal to the previously accepted parameter and a standard deviation equal to a fraction of the initial parameter range. The standard deviation was adjusted to achieve an acceptance rate of 25 – 30% and to prevent the routine from getting stuck at local minima. Parameters that fell outside of their data-informed prior range were re-drawn. The parameter space was explored for 50,000 iterations. The best parameter set was the one that minimized the overall cost function (*J*, equation 11). This overall cost function treats all data streams equally and values relative improvements in goodness-of-fit (Franks et al., 1999, Richardson et al., 2010).

$$J = \prod_{i} j_i$$ **Equation 11**

Step two estimated parameter uncertainty by exploring the parameter set that yielded the smallest value for *J* in step one. Parameter values were drawn from a normal distribution with a mean equal to the best parameter set from step one and the standard deviation from the end of step one. Uncertainty weighted data-model disagreements were normalized based on the variance of the *j*'s obtained in step one. Parameter sets were accepted if the cost function for each data stream (j_i) passed a chi-squared test (CI = 90%) (Franks et al., 1999, Richardson et al., 2010, Keenan et al.,

2012a, Wright and Rocha, 2018). Step two yielded 10,000 accepted parameter sets, chosen to balance the need to capture the distribution of tussock sizes and the computational time.

We assessed parameter sensitivity by plotting LOESS smoothed predicted radius at 250 years for the parameter sets obtained in step two versus the parameters used in those predictions. The difference in LOESS smoothed predicted tussock radius at 250 years for the minimum and maximum parameter sets obtained in step two was used as a sensitivity measure. We also manipulated the constrained model by making predictions with tiller radius altered to extremely large (0.64 cm) and extremely small (0 cm) values to demonstrate the impact of different parameters and processes on the model predictions.

3. Results

3.1 In-situ tussock development and size

Tussock development and size were mostly dependent on disturbance history and tussock age, and less so on environmental conditions. At the disturbed Eagle creek bladed (EC-B) site with young tussocks, averaged tussock radius significantly increased at a rate of 0.25 ± 0.06 cm y^{-1} ($P<0.001$; Figure 3a). At the undisturbed sites with older tussocks (EC-U, CT-1, CT-2), site averaged tussock radius either remained unchanged or slightly declined (Figure 3b). Across the North Slope, site averaged tussock radius was relatively constant and only weakly related to climate (Figure S5; Table S1). Average growing season temperature only explained 15% of the variation in site averaged tussock radius, while annual precipitation explained only 9% of the

variation in site averaged tussock radius. This relationship was weak despite a latitudinal decline of 2.2 ^{o}C and 178 mm of precipitation across the measured sites.

3.2 Tussock development and size model dynamics

The impacts of hexagonal packing and limited carrying capacity for new tillers on tussock development were illustrated using the best fit parameter values for the model with modifications to tiller size (Figure 4). Unrealistically small tillers minimized the impact of packing on reproduction resulting in exponential tussock growth, while unrealistically large tillers enhanced the impact of tiller packing on reproduction and resulted in tussocks that were unable to grow. Best fit tiller size fell in between these two extremes and resulted in tussocks that grew rapidly and approached steady-state size within 50 years (Figure 4).

Steady-state tussock size depended on the tussock's mass balance (Figure 5a). Initially, tussock size increases when necromass gains exceeded necromass losses. Steady-state tussock size was reached when tussock mass gains equaled mass losses. This occurred when the packing index reached 1, indicating that there was insufficient space for new tillers, and tiller reproduction declined. Space limitation and declining tiller reproduction rates eventually stabilized the proportion of living and dead tillers atop the tussock (Figure 5b).

3.3 Model parameterization with model data fusion

Model data fusion constrained the parameters of the tussock development model within the ranges observed in the field. The posterior parameter distributions largely overlapped the observed parameter distributions (Figure 6). In some cases, the average for the posterior

distribution was slightly higher than for the observed distribution, especially for tiller radius and the root input rate per tiller. This was likely due to measurement limitations or simplifications that were made to processes in the model. For example, the observed distribution for tiller radius was informed by a mix of young and old tillers that differ in radius due to litter accumulation. Consequently, the larger posterior tiller radius mean likely better represents older accumulated tillers rather than younger recently developed tillers. Lastly, the posterior mean tiller root productivity represents a lifetime average, and it is expected that interannual climate variability will alter the mean of the prior probability distribution within the constrained range of values specified by the observations.

Model-data fusion constrained the posterior parameter distributions with reductions in the interquartile range (IQR) and a shift towards roughly normal probability distributions (Table 1; Figure 6). The IQR for the dead tiller decomposition and removal rate decreased the most (25% of prior IQR), whereas the IQR for the root input rate per tiller decreased the least (44% of prior IQR). Five of the seven fitted parameters were strongly identifiable (i.e. they could be constrained by the model data fusion) and weakly correlated during the model data fusion (Figure S6; Table S2). The two remaining parameters, the root necromass decomposition rate and the dead tiller decomposition and removal rate were positively correlated and therefore more difficult to constrain. Nonetheless, the model-data fusion constrained their IQRs and yielded distributions that closely overlapped those observed in the field (Figure 6).

The model data fusion fitted parameters were able to replicate the observed distribution of tussock size, as well as the allometric relationship between tussock radius, number of living

tillers, and necromass. The model predictions of tussock radius replicated those observed across the North Slope with the predicted distribution overlapping 95% of the observed distribution (Figure 7a). Modeled tussock radius ranged from 0.2 to 14 cm with a mean of 6 cm, while observed tussock radius ranged from 0.05 to 30 cm with a mean of 7 cm. Tussocks at the high and low end of the distributions were less represented by the model. The model captured the non-linear root necromass and tussock radius allometry with the measured and modeled uncertainties overlapping for 86% of the observations (Figure 7b). The model also captured the non-linear living tillers and tussock radius allometry with the measured and modeled uncertainties overlapping for 97% of the observations (Figure 7c).

3.4 Tussock size sensitivity analyses

Sensitivity analysis of the constrained model quantified the importance of each model parameter in determining steady-state tussock size (Figure 8). Physical parameters had the highest average sensitivity, and demographic parameters had the lowest average sensitivity. In order from strongest to weakest sensitivity for physical factors, the root input rate per tiller was positively related to tussock radius, and the root necromass decomposition rate and the dead tiller decomposition and removal rate were negatively related to tussock radius. For structural factors root necromass bulk density and tiller radius were both negatively related to tussock radius. For demographic factors, the per-capita birth rate, the initial per-capita death rate, and the initial per-capita population growth rate were all negatively related to tussock radius. The highest overall sensitivity was associated with the root input rate per tiller with an 8.2 cm change in predicted steady-state tussock size across the constrained parameter distribution. The second highest

overall sensitivity was associated with root necromass bulk density with a 6.6 cm change in predicted steady-state tussock size across the constrained parameter distribution.

3.5 Insights into steady-state tussock size

The model sensitivity analyses provided hypotheses that were independently tested with observations. We corroborated the predicted sensitivity of tussock size to the most important measurable parameter in each category with observations. The independent field observations in Figure 9 mirrored the model sensitivity predictions in Figure 8. Tiller root productivity was positively related to tussock radius in tussocks measured in the field ($y = 3.5 \pm 1.0 + 79x \pm 14$, $P < 0.001$, $R^2 = 0.5$; Figure 9a). Root necromass bulk density was negatively related to tussock radius ($y = 11.1 \pm 1.4 - 18.8x \pm 7.2$, $P = 0.014$, $R^2 = 0.17$; Figure 9b). Tiller reproduction exhibited a weak negative relationship with tussock radius ($y = 10.41 \pm 1.6 -9.02x \pm 5.18$; $P = 0.09$, $R^2 = 0.08$; Figure 9c). The relative importance of these factors in controlling tussock size mirrored that of the model sensitivity analysis, as indicated by their R^2 and slopes. The observed relationship between tiller root productivity and tussock size had the highest R^2 and slope, whereas tiller reproduction and tussock size had the lowest R^2 and slope. The parallels between the constrained model sensitivities and the field observations were surprising, given that the model was only constrained using the tussock size distribution, and the relationship between tussock radius, number of living tillers, and necromass. These parallels provide further validation of the model's predictive ability since they emerged independently from the mathematical representation of tussock development.

4. Discussion

Insights into the controls on tussock size were possible through model-data fusion and sensitivity analysis of the constrained model. Model data fusion provided biological constraints for realistic predictions of tussock size (Table 1; Figure 6, 7). These constraints were necessary for the model to reflect field observations of rapid growth in young tussocks and growth declines in mature tussocks (Figure 3). For example, the model demonstrated that tussocks grew exponentially without the assumption of hexagonal packing and density-dependent reproduction (Figure 4). Synthesis of model dynamics and observations indicated that site averaged tussock size was attributed to intrinsic physical and structural controls, rather than extrinsic environmental controls (Figure 3, 4, 5, 8). These intrinsic controls manifested through feedbacks between tussock necromass balance, available carrying capacity for new tillers, and density-dependent reproduction (Figure 4, 5, 8). The model sensitivity analyses illustrated the importance of these feedbacks and provided hypotheses about the main controls of tussock size that were independently validated with field data (Figure 8, 9).

4.1 What controls steady state tussock size?

Sensitivity analyses of the constrained model demonstrated that steady state tussock size was largely controlled by both physical and structural factors, and less so by demographic factors. This intuitively makes sense given the feedback between tussock necromass balance, available carrying capacity, and density-dependent reproduction. The model explicitly links the carrying capacity (K_A) to the amount of unoccupied space on top of the tussock through hexagonal tiller packing. Tussock growth only occurred when its mass balance was positive, resulting in increased carrying capacity for new tillers and greater root productivity to offset increasing decomposition losses from the larger necromass stock. As tussocks aged, the population of dead

tillers increased, the total proportion of living tillers decreased, and cumulative decomposition increased due to the increased size of the necromass pool. As a result, greater tiller root production was needed to compensate for increasing decomposition losses in larger tussocks for tussocks to maintain a positive mass balance. The model also points to an important structural property where a longer positive mass balance and larger tussock can be achieved by reducing the structural requirement for the necromass pool through decreases in bulk density. This process is consistent with the idea that the tussock mound microenvironment sustains the population of tillers atop the tussock (Lawrence and Zedler, 2011, Crain and Bertness, 2005, Chapin et al., 1979, Doust, 1981, Oliva et al., 2005). It is also consistent with the complex observed patterns of tiller population density, tussock radius, and tiller reproduction rates in tussock cottongrass including a shift from high tiller reproduction rates in younger, smaller less densely packed tussock to lower reproduction rates in older more densely packed tussocks (Fetcher and Shaver, 1982, Fetcher, 1985, Fetcher and Shaver, 1983). The role of these processes in controlling tussock development is further supported by the corroboration of the tussock size model parameter sensitivities with observations (Figures 8,9). Such strong agreement indicates that the tussock model provided accurate insight into the controls on tussock development and size.

4.2 Could latent factors provide alternate explanations for tussock size controls?

Latent factors are those factors that were excluded from the mathematical model but may be important for tussock growth and size. Soil anoxia with increasing tussock size increased nutrient limitation with increasing tussock size, or signaling due to a reduction in the red to far red ratio with increasing tiller density are three possible latent factors. Tussock necromass has a high moisture holding capacity that may induce anoxic conditions and decrease tiller root productivity

in large tussocks (Gebauer et al., 1996, Stuart and Miller, 1982a, Stuart and Miller, 1982b). However, both our field observations and the model sensitivity analysis exhibit the opposite pattern with a positive relationship between tiller root productivity and tussock size. Nutrient limitation also could constrain tussock size by 1) reducing tiller root input, 2) increasing tiller death rates, or 3) reducing tiller reproduction rates (Chapin et al., 1988, Chapin et al., 1979, Shaver et al., 1986b). Factors 1 and 2 were deemed unimportant, given the strong positive relationship between root input rate per tiller and tussock size (Figures 8,9) and the weak negative relationship between the initial per-capita death rate and tussock size (Figure 8). In regards to the third factor, the model incorporates previous work that demonstrates a decrease in tiller birth rates with increasing tussock size (Fetcher and Shaver, 1982, Fetcher, 1985, Fetcher and Shaver, 1983). A reduction in the red to far red ratio due to increased tiller density which leads to signaling by phytochrome would similarly decrease tiller birth rates with increasing tussock size (de Kroon and Kwant, 1991, de Kroon, 1993, Deregibus et al., 1983, Fetcher, 1985, Deregibus et al., 1985). Declining tiller birth rates in larger tussocks were represented in the model through hexagonal tiller packing and density-dependent reproduction. Therefore, we argue that the model may be capturing these growth dynamics without explicitly representing nutrient limitation or changes in the red to far red ratio.

4.3 Conclusion

We presented a case study that integrated models and data to develop mechanistic insights into the complex long-term controls on an important foundation species in rapidly changing Arctic ecosystems. These insights include the importance of belowground C allocation in regulating tussock size, and the intrinsic physical and structural controls on tussock C accumulation. The

results imply that future climate change is unlikely to affect the intrinsic control on tussock cottongrass size, so future work should focus on factors regulating its abundance across the arctic. The model could inform the representation of tussocks in terrestrial biosphere models allowing tussock-forming processes to be included in ecosystems where they are present. This is particularly relevant to the Arctic where tussocks will influence the ecosystem's response to climate change. The tussock model also provides an opportunity to determine whether the mechanisms regulating tussock size are similar across other tussock grass and sedge species, given the large variation in tussock size that occurs across grasses and sedges. These insights will facilitate a better understanding of the current and future role of tussocks in regulating ecosystem structure and function.

Data Availability Statement

The data and code which support this study are archived on Zenodo at https://doi.org/10.5281/zenodo.6896732.

Acknowledgments

Thanks to G. Shaver for your helpful comments and R. An, B. Blakely, D. Dech, C. Hammack, N. Ho, I. Klupar, H. Long, M. Melendez, E. Niklinska, S. Unger, C. Vizza, M. Williams, and N. Zimov, for their assistance. This work was supported by the National Science Foundation (DEB 1556772 to A.V.R., DGE 1841556 to S.R.C., PLR 1418010 to N.F.), the University of Notre Dame, Fulbright (open study/research grant to S.R.C.), and National Geographic (Young explorer grant to S.R.C). We also thank the Toolik field station, the Arctic LTER (NSF/PLR 1637459), the North East Science Station, and BP Exploration Alaska.

Author contributions

S.R.C. and A.V.R. conceived the research. S.R.C, N.F., D. P. W., and A.V. R. collected the field data. S.R.C, K. S. W., and A. V. R. designed and conducted the modeling analysis. All authors contributed to data interpretation and preparation of the manuscript text.

Figures

Figure 1: An artist's depiction of a cross-section of *Eriophorum vaginatum's* tussock growth form.

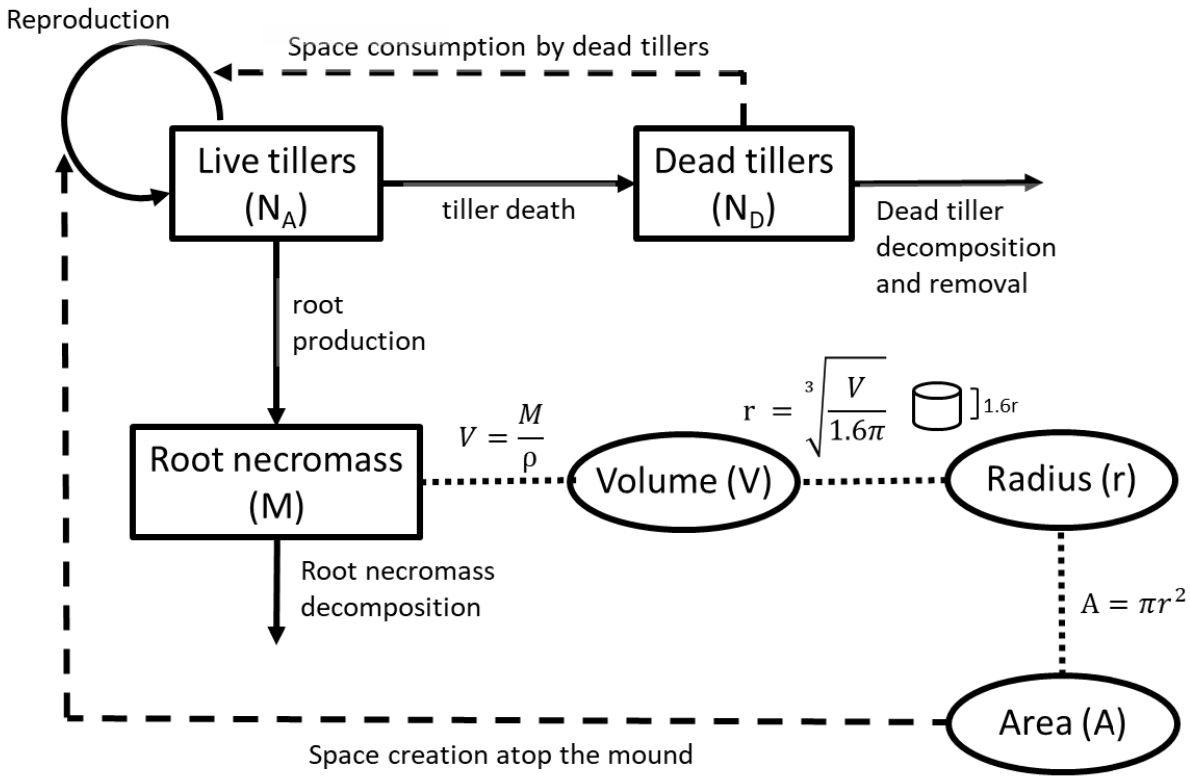

Figure 2: A conceptual diagram of our tussock growth model. Boxes represent state variables, solid lines represent flows of material, circles represent derived quantities, dotted lines represent the calculation of a derived quantity, and dashed lines represent constraints.

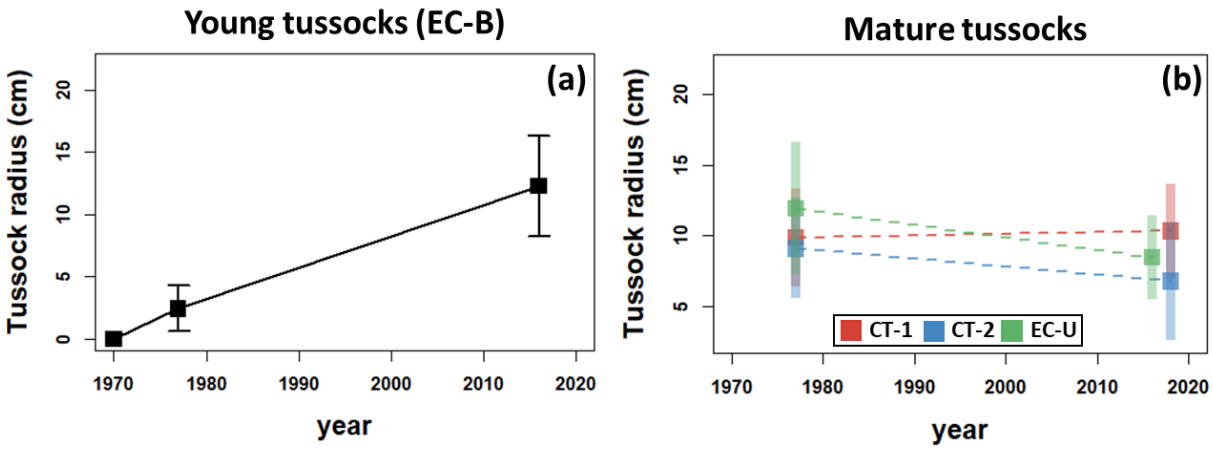

Figure 3. Temporal dynamics in site averaged tussock radius at **a)** the disturbed Eagle creek bladed site with young tussocks (EC-B). and at **b)** the Cape Thompson 1 and 2 (CT-1/2) and Eagle creek undisturbed (EC-U) sites with old tussocks. Bars represent standard deviations.

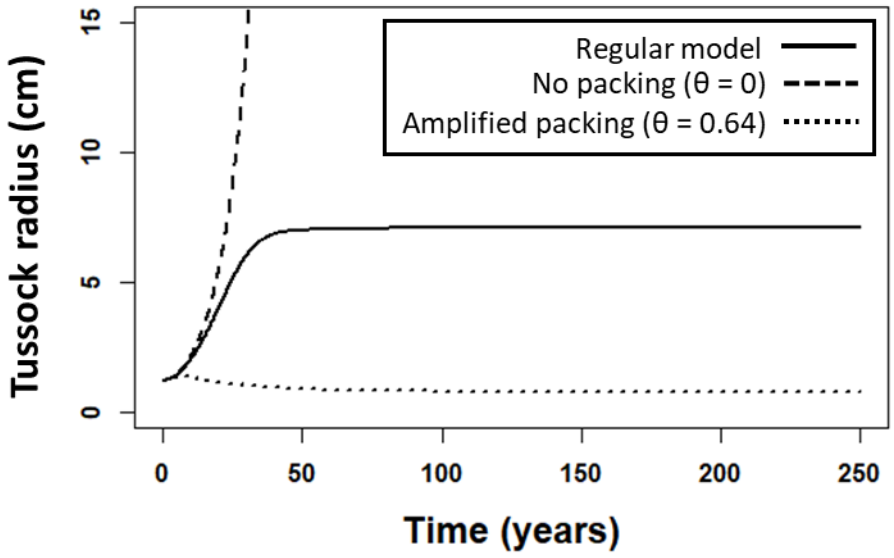

Figure 4. Temporal dynamics of tussock growth as influenced by extremely small- (hatched line), medium-(solid line), and extremely large- (dotted line) sized tillers.

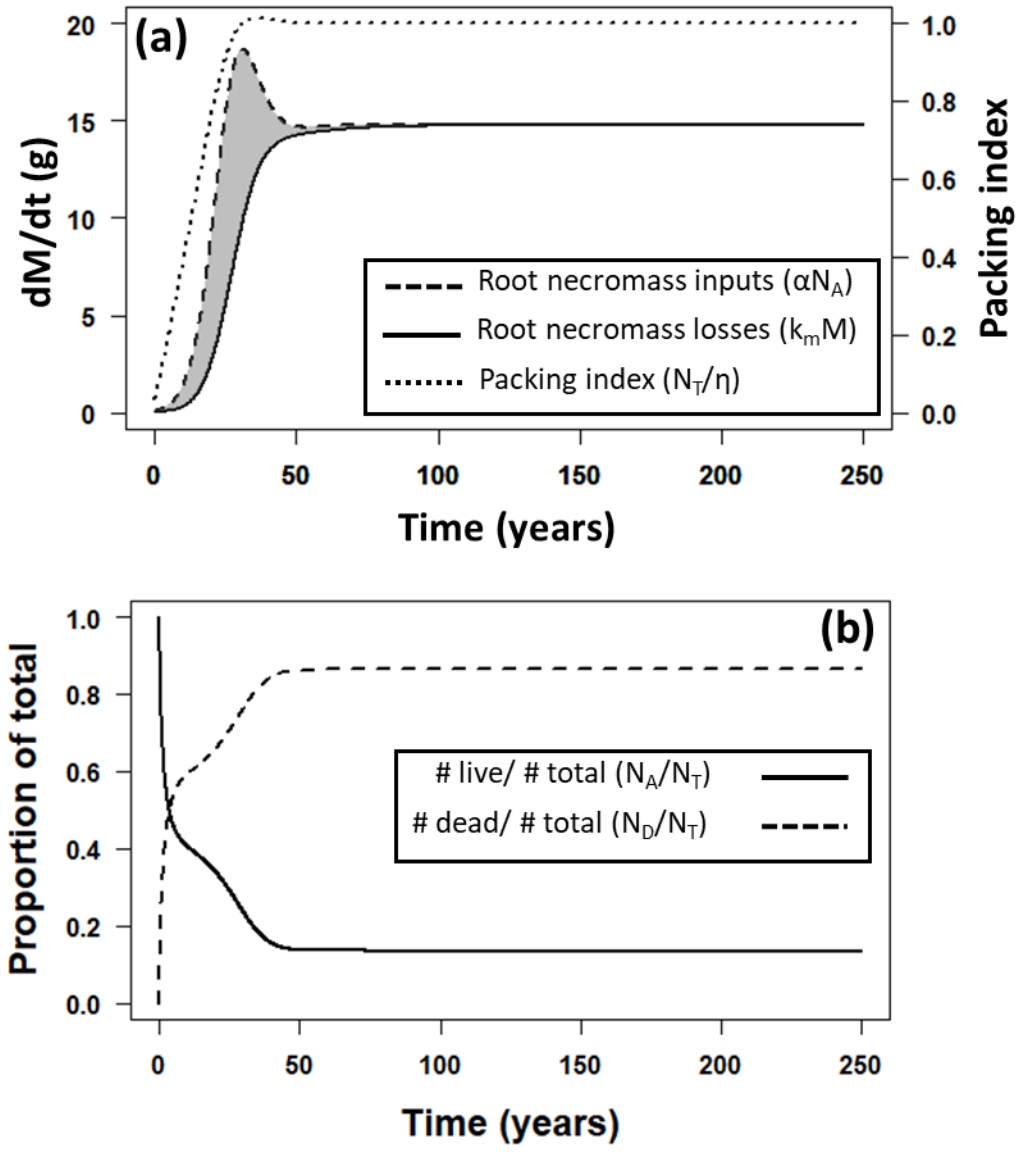

Figure 5. Temporal dynamics of **a)** the components of necromass balance and packing index, and **b)** the proportional of the total population composed of living (solid line) and dead (hatched line) tillers atop the tussock using the best-fit parameters. In the a panel tussock mass inputs are represented by a hatched line, mass outputs are represented by a solid line, and the packing index is represented by a dotted line. The shaded gray area denotes a positive tussock mass balance and associated tussock growth.

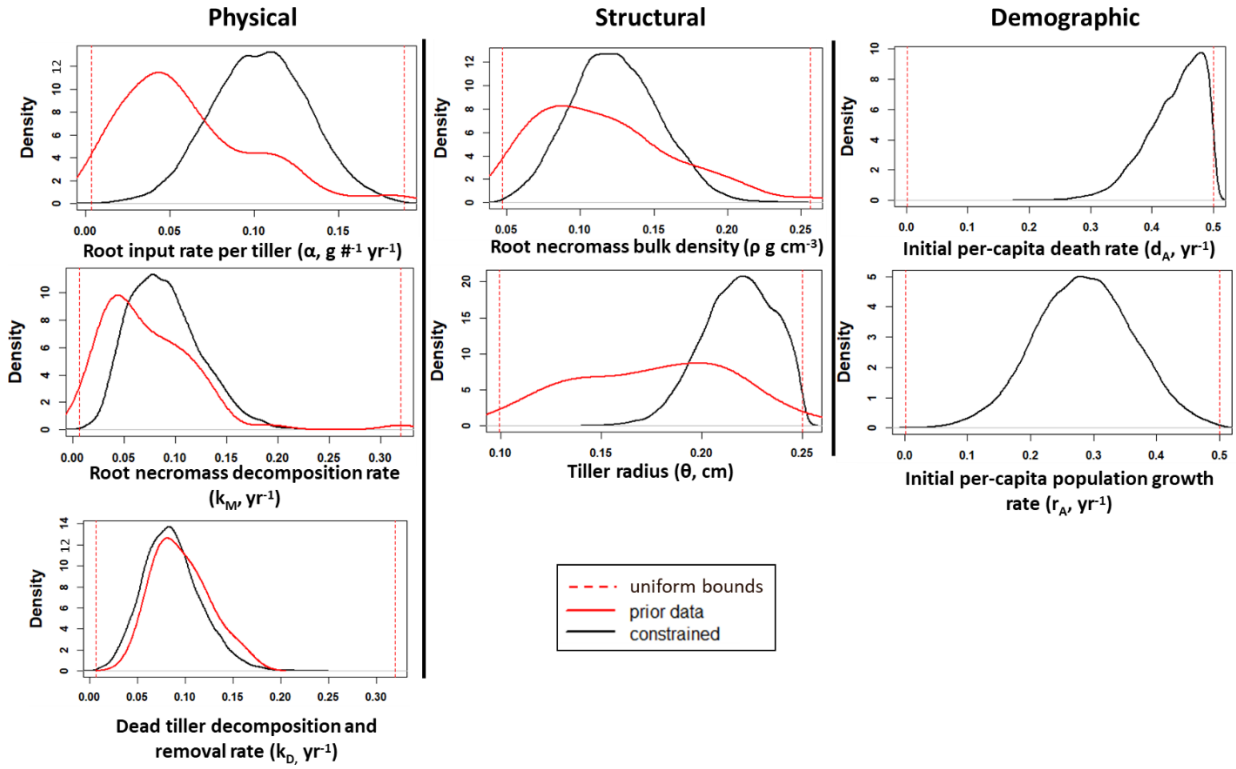

Figure 6: Prior (red) and posterior (black) probability distributions for the tussock size model parameters fitted with model data fusion.

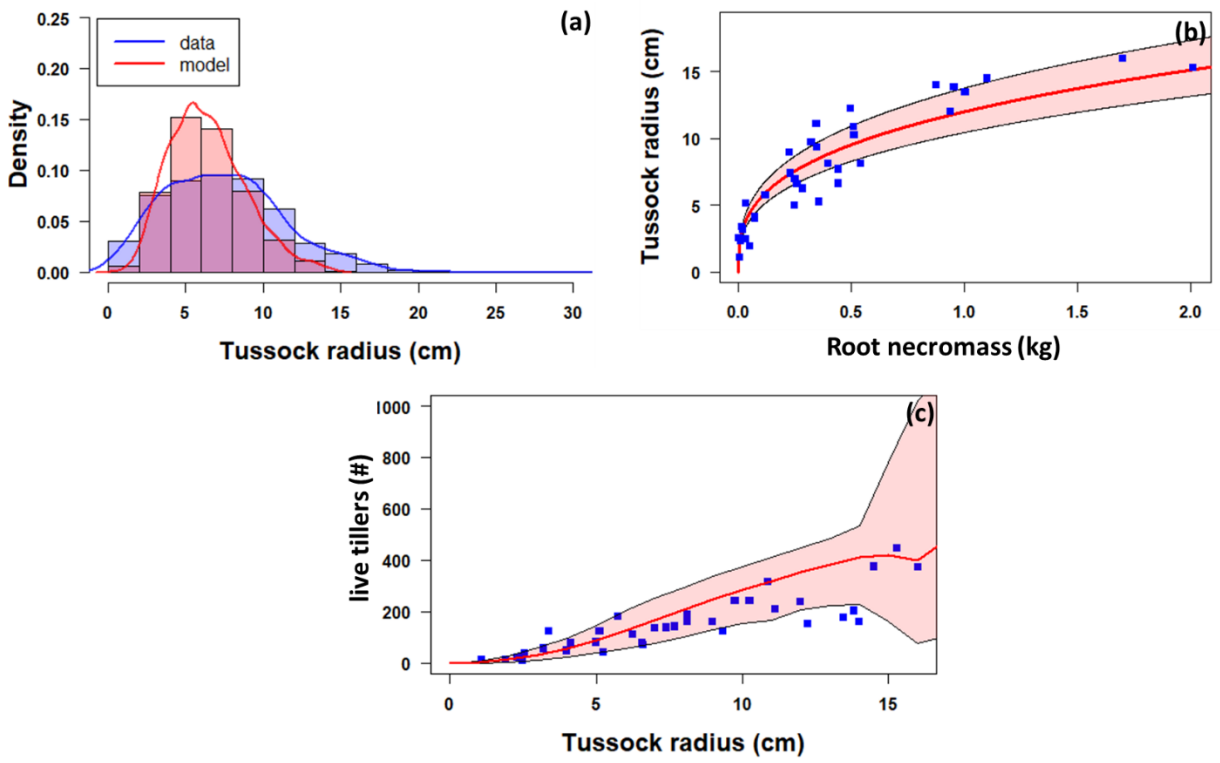

Figure 7. Model and data comparisons of **a)** the tussock radius probability distributions, **b)** the relationship between root necromass and tussock radius, and **c)** the relationship between the number of living tillers and tussock radius. The shaded red region in panels b and c represented the 90% confidence interval for model predictions.

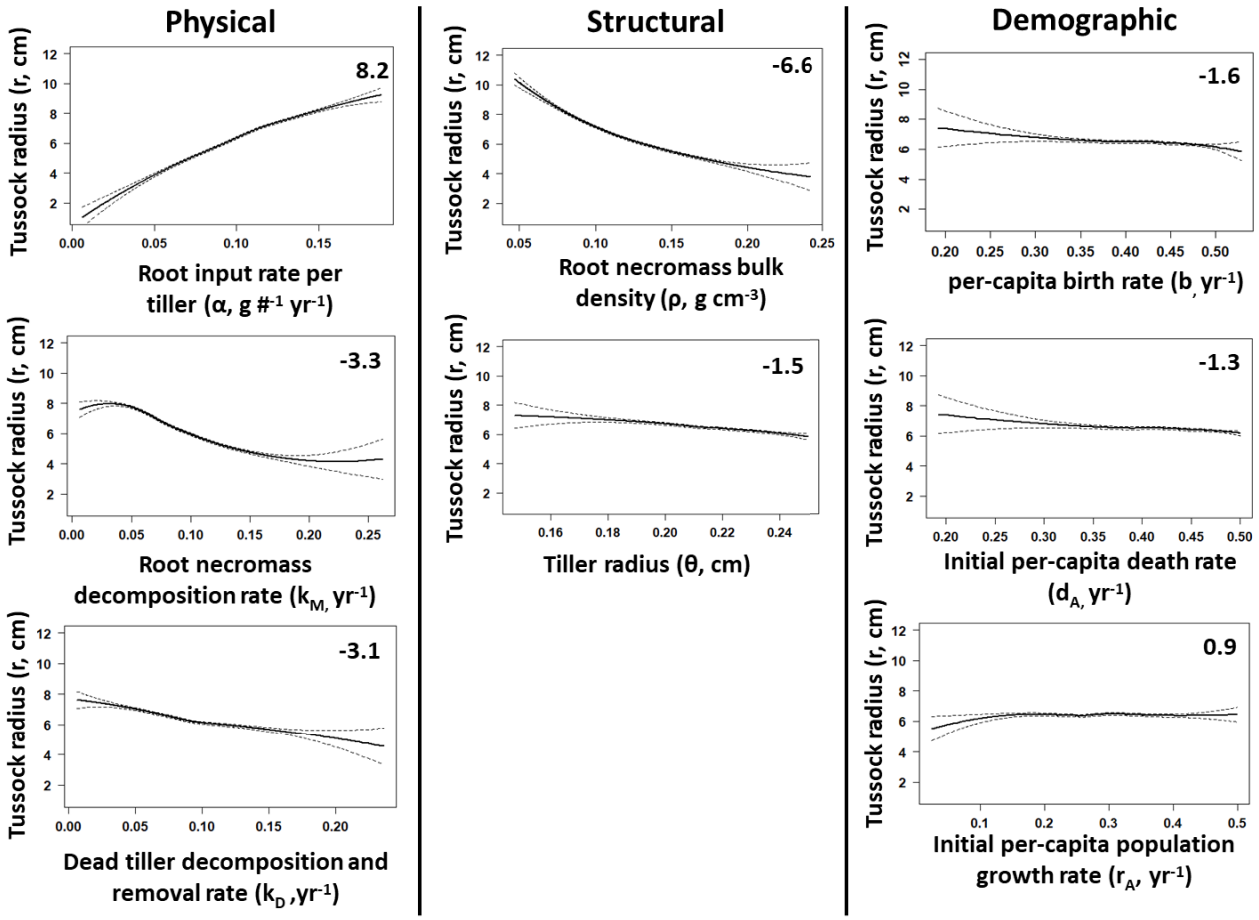

Figure 8: Tussock radius sensitivity to the model parameters with 95% confidence intervals. The parameter sensitivity as shown in the upper right corner is quantified as the difference in average tussock radius after 250 years between the lowest and highest value in the parameter distribution.

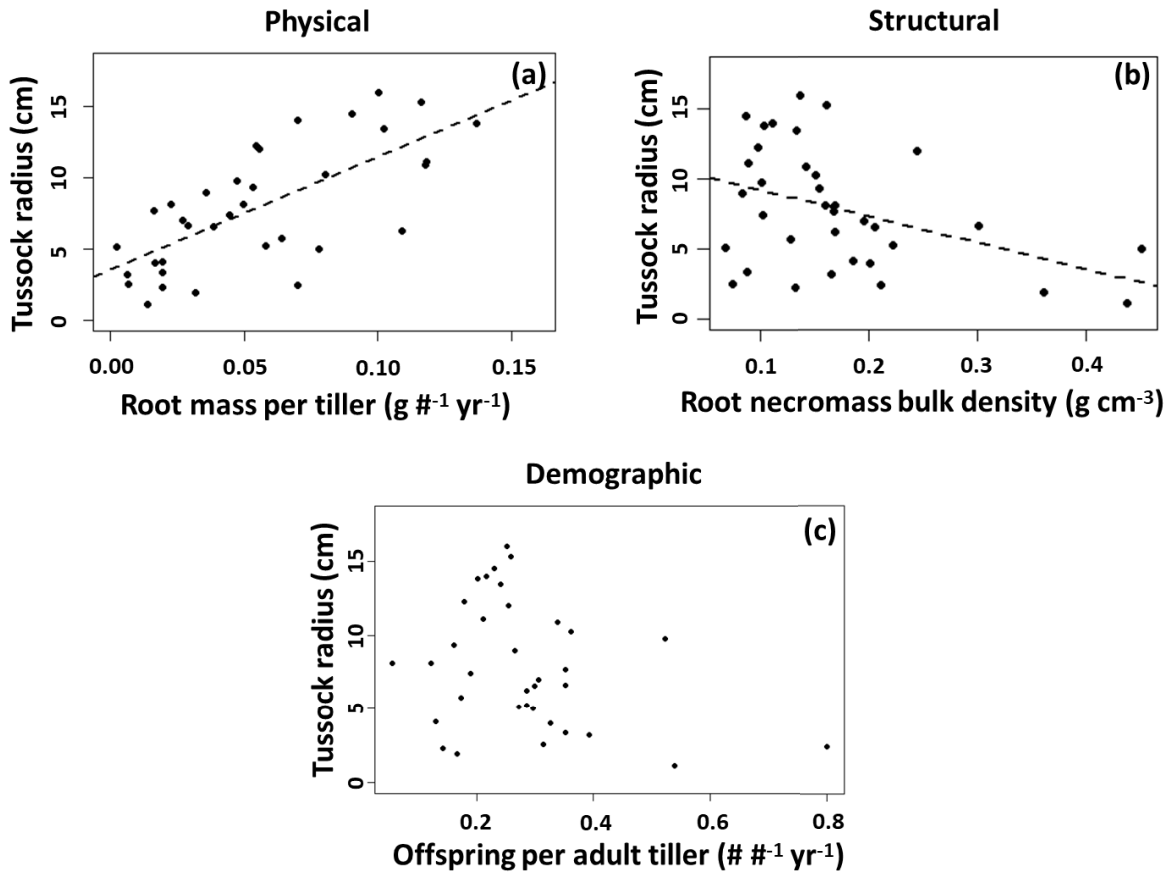

Figure 9: Observed relationships between **a)** tiller root productivity and tussock radius**, b)** root necromass bulk density and tussock radius, and **c)** offspring per adult tiller observed in harvested tussocks versus tussock radius. Statistically significant relationships at the 95% confidence level are denoted with a hatched regression line.

Tables

Table 1. Description of state variables, free parameters, and other derived values. Prior ranges best fit model parameters and the percentage of the prior interquartile range are included for free parameters.

Name	Symbol	Units	Prior (min, max)	Best fit	% of prior IQR
		State variables			
Live tillers	N_A	#	-	-	-
Dead tillers	N_D	#	-	-	-
Root necromass	M	g	-	-	-
		Free parameters			
Root necromass bulk density	ρ	g cm^{-3}	0.05, 0.26[1]	0.11	39%
Tiller radius	θ	cm	0.1, 0.25[1]	0.21	32%
Root input rate per tiller	α	g $\#^{-1}$ yr^{-1}	0.003, 0.19[1]	0.11	44%
Root necromass decomposition rate	k_M	yr^{-1}	0.006, 0.32[1]	0.07	31%
Initial per-capita population growth rate	r_A	yr^{-1}	0.001, 0.5[2]	0.28	43%
Initial per-capita death rate	d_A	yr^{-1}	0.001, 0.5[2]	0.48	27%
Dead tiller decomposition and removal rate	k_D	yr^{-1}	0.006, 0.32[1]	0.08	25%
		Other			
Carying capacity for live tillers	K_A	#	-	-	-
Tussock radius	r	cm	-	-	-
Tussock volume	V	cm^3	-	-	-
Per-capita birth rate	b	yr^{-1}	-	-	-

See [1]2.3 Tussock allometry, tiller characteristics, and decomposition, [2]Fetcher and Shaver (1983).

References

ANDREN, O. & PAUSTIAN, K. 1987. Barley straw decomposition in the field: a comparison of models. *Ecology,* 68**,** 1190-1200.

ANTONOVICS, J. & LEVIN, D. A. 1980. The ecological and genetic consequences of density-dependent regulation in plants. *Annual Review of Ecology and Systematics,* 11**,** 411-452.

BALKE, T., KLAASSEN, P. C., GARBUTT, A., VAN DER WAL, D., HERMAN, P. M. & BOUMA, T. J. 2012. Conditional outcome of ecosystem engineering: A case study on tussocks of the salt marsh pioneer Spartina anglica. *Geomorphology,* 153**,** 232-238.

BARKHAM, J. & HANCE, C. 1982. Population Dynamics of the Wild Daffodil (Narcissus Pseudonarcissus): III. Implications of a Computer Model of 1000 Years of Population Change. *The Journal of Ecology***,** 323-344.

BELL, A. 1979. The hexagonal branching pattern of rhizomes of Alpinia speciosa L.(Zingiberaceae). *Annals of Botany,* 43**,** 209-223.

BENNINGTON, C. C., FETCHER, N., VAVREK, M. C., SHAVER, G. R., CUMMINGS, K. J. & MCGRAW, J. B. 2012a. Home site advantage in two long-lived arctic plant species: results from two 30-year reciprocal transplant studies. *Journal of Ecology,* 100**,** 841-851.

BENNINGTON, C. C., FETCHER, N., VAVREK, M. C., SHAVER, G. R., CUMMINGS, K. J. & MCGRAW, J. B. 2012b. Home site advantage in two long-lived arctic plant species: results from two 30-year reciprocal transplant studies. *Journal of Ecology,* 100**,** 841-851.

BENSCOTER, B. W. & VITT, D. H. 2008. Spatial patterns and temporal trajectories of the bog ground layer along a post-fire chronosequence. *Ecosystems,* 11**,** 1054-1064.

BEVEN, K. 2006. A manifesto for the equifinality thesis. *Journal of hydrology,* 320**,** 18-36.

BOX, J. E., COLGAN, W. T., CHRISTENSEN, T. R., SCHMIDT, N. M., LUND, M., PARMENTIER, F.-J. W., BROWN, R., BHATT, U. S., EUSKIRCHEN, E. S., ROMANOVSKY, V. E., WALSH, J. E., OVERLAND, J. E., WANG, M., CORELL, R. W., MEIER, W. N., WOUTERS, B., MERNILD, S., MÅRD, J., PAWLAK, J. & OLSEN, M. S. 2019. Key indicators of Arctic climate change: 1971–2017. *Environmental Research Letters,* 14.

CHAPIN, F. S., FETCHER, N., KIELLAND, K., EVERETT, K. R. & LINKINS, A. E. 1988. Productivity and nutrient cycling of Alaskan tundra: enhancement by flowing soil water. *Ecology,* 69**,** 693-702.

CHAPIN, F. S., VAN CLEVE, K. & CHAPIN, M. C. 1979. Soil temperature and nutrient cycling in the tussock growth form of Eriophorum vaginatum. *The Journal of Ecology***,** 169-189.

CRAIN, C. M. & BERTNESS, M. D. 2005. Community impacts of a tussock sedge: is ecosystem engineering important in benign habitats? *Ecology,* 86**,** 2695-2704.

CURASI, S. R., FETCHER, N., HEWITT, R. E., LAFLEUR, P. M., LORANTY, M. M., MACK, M. C., MAY, J. L., MYERS-SMITH, I. H., NATALI, S. M. & OBERBAUER, S. F. 2022. Range shifts in a foundation sedge potentially induce large Arctic ecosystem carbon losses and gains. *Environmental Research Letters,* 17**,** 045024.

CURASI, S. R., PARKER, T. C., ROCHA, A. V., MOODY, M. L., TANG, J. & FETCHER, N. 2019. Differential responses of ecotypes to climate in a ubiquitous Arctic sedge: implications for future ecosystem C cycling. *New Phytol*.

DARWIN, C. 1859. *On the origin of species by means of natural selection, or, The preservation of favoured races in the struggle for life*, London : J. Murray.

DE KROON, H. 1993. Competition between shoots in stands of clonal plants. *Plant Species Biology,* 8**,** 85-94.

DE KROON, H. & KWANT, R. 1991. Density-dependent growth responses in two clonal herbs: regulation of shoot density. *Oecologia,* 86**,** 298-304.

DEREGIBUS, V., SANCHEZ, R., CASAL, J. & TRLICA, M. 1985. Tillering responses to enrichment of red light beneath the canopy in a humid natural grassland. *Journal of applied Ecology*, 199-206.

DEREGIBUS, V. A., SANCHEZ, R. A. & CASAL, J. J. 1983. Effects of light quality on tiller production in Lolium spp. *Plant physiology,* 72, 900-902.

DERNER, J. D., BRISKE, D. D. & POLLEY, H. W. 2012. Tiller organization within the tussock grass Schizachyrium scoparium: a field assessment of competition–cooperation tradeoffs. *Botany,* 90, 669-677.

DIETZE, M. C., LEBAUER, D. S. & KOOPER, R. 2013. On improving the communication between models and data. *Plant, Cell & Environment,* 36, 1575-1585.

DOUST, L. L. 1981. Population dynamics and local specialization in a clonal perennial (Ranunculus repens): I. The dynamics of ramets in contrasting habitats. *The Journal of Ecology*, 743-755.

ELDRIDGE, D. J., BOWKER, M. A., MAESTRE, F. T., ALONSO, P., MAU, R. L., PAPADOPOULOS, J. & ESCUDERO, A. 2010. Interactive effects of three ecosystem engineers on infiltration in a semi-arid Mediterranean grassland. *Ecosystems,* 13, 499-510.

ELUMEEVA, T. G., ONIPCHENKO, V. G. & WERGER, M. J. 2017. No other species can replace them: evidence for the key role of dominants in an alpine Festuca varia grassland. *Journal of Vegetation Science,* 28, 674-683.

FETCHER, N. 1983. Optimal life-history characteristics and vegetative demography in Eriophorum vaginatum. *The Journal of Ecology*, 561-570.

FETCHER, N. 1985. Effects of removal of neighboring species on growth, nutrients, and microclimate of Eriophorum vaginatum. *Arctic and Alpine Research,* 17, 7-17.

FETCHER, N. & SHAVER, G. 1983. Life histories of tillers of Eriophorum vaginatum in relation to tundra disturbance. *Journal of Ecology,* 71, 131-147.

FETCHER, N. & SHAVER, G. R. 1982. Growth and tillering patterns within tussocks of Eriophorum vaginatum. *Ecography,* 5, 180-186.

FICK, S. E. & HIJMANS, R. J. 2017. WorldClim 2: new 1-km spatial resolution climate surfaces for global land areas. *International journal of climatology,* 37, 4302-4315.

FRANKS, S. W., BEVEN, K. J. & GASH, J. H. 1999. Multi-objective conditioning of a simple SVAT model.

GEBAUER, R. L., TENHUNEN, J. D. & REYNOLDS, J. F. 1996. Soil aeration in relation to soil physical properties, nitrogen availability, and root characteristics within an arctic watershed. *Plant and Soil,* 178, 37-48.

HOBBIE, J. E., SHAVER, G. R., RASTETTER, E. B., CHERRY, J. E., GOETZ, S. J., GUAY, K. C., GOULD, W. A. & KLING, G. W. 2017. Ecosystem responses to climate change at a Low Arctic and a High Arctic long-term research site. *Ambio,* 46, 160-173.

KARBERG, N. J., SCOTT, N. A. & GIARDINA, C. P. 2008. Methods for estimating litter decomposition. *Field measurements for forest carbon monitoring.* Springer.

KEENAN, T., BAKER, I., BARR, A., CIAIS, P., DAVIS, K., DIETZE, M., DRAGONI, D., GOUGH, C. M., GRANT, R. & HOLLINGER, D. 2012a. Terrestrial biosphere model performance for inter-annual variability of land-atmosphere CO2 exchange. *Global Change Biology,* 18, 1971-1987.

KEENAN, T. F., CARBONE, M. S., REICHSTEIN, M. & RICHARDSON, A. D. 2011. The model–data fusion pitfall: assuming certainty in an uncertain world. *Oecologia,* 167, 587.

KEENAN, T. F., DAVIDSON, E., MOFFAT, A. M., MUNGER, W. & RICHARDSON, A. D. 2012b. Using model-data fusion to interpret past trends, and quantify uncertainties in future projections, of terrestrial ecosystem carbon cycling. *Global Change Biology,* 18, 2555-2569.

KYKER-SNOWMAN, E., LOMBARDOZZI, D. L., BONAN, G. B., CHENG, S. J., DUKES, J. S., FREY, S. D., JACOBS, E. M., MCNELLIS, R., RADY, J. M. & SMITH, N. G. 2022. Increasing the spatial and temporal impact of ecological research: A roadmap for integrating a novel terrestrial process into an Earth system model. Wiley Online Library.

LAWRENCE, B. A. & ZEDLER, J. B. 2011. Formation of tussocks by sedges: effects of hydroperiod and nutrients. *Ecological Applications,* 21**,** 1745-1759.
LAWRENCE, B. A. & ZEDLER, J. B. 2013. Carbon storage by Carex stricta tussocks: a restorable ecosystem service? *Wetlands,* 33**,** 483-493.
LONSDALE, W. & WATKINSON, A. 1983. Tiller dynamics and self-thinning in grassland habitats. *Oecologia,* 60**,** 390-395.
MA, T., PARKER, T., FETCHER, N., UNGER, S. L., GEWIRTZMAN, J., MOODY, M. L. & TANG, J. 2022. Leaf and root phenology and biomass of Eriophorum vaginatum in response to warming in the Arctic. *Journal of Plant Ecology*.
MACANDER, M. J., NELSON, P. R., NAWROCKI, T., FROST, G. V., ORNDAHL, K., PALM, E. C., WELLS, A. F. & GOETZ, S. J. 2022. Time-series maps reveal widespread change in plant functional type cover across arctic and boreal Alaska and Yukon. *Environmental Research Letters*.
MARK, A. F., FETCHER, N., SHAVER, G. R. & III, F. S. C. 1985. Estimated Ages of Mature Tussocks of Eriophorum vaginatum along a Latitudinal Gradient in Central Alaska, U.S.A. *Arctic and Alpine Research,* 17.
MCGRAW, J. B., TURNER, J. B., SOUTHER, S., BENNINGTON, C. C., VAVREK, M. C., SHAVER, G. R. & FETCHER, N. 2015. Northward displacement of optimal climate conditions for ecotypes of Eriophorum vaginatum L. across a latitudinal gradient in Alaska. *Glob Chang Biol,* 21**,** 3827-35.
NAZZI, F. 2016. The hexagonal shape of the honeycomb cells depends on the construction behavior of bees. *Scientific reports,* 6**,** 1-6.
OBORNY, B., MONY, C. & HERBEN, T. 2012. From virtual plants to real communities: a review of modelling clonal growth. *Ecological Modelling,* 234**,** 3-19.
OLIVA, G., COLLANTES, M. & HUMANO, G. 2005. Demography of grazed tussock grass populations in Patagonia. *Rangeland Ecology & Management,* 58**,** 466-473.
PARKER, T. C., SANDERMAN, J., HOLDEN, R. D., BLUME-WERRY, G., SJÖGERSTEN, S., LARGE, D., CASTRO-DÍAZ, M., STREET, L. E., SUBKE, J. A. & WOOKEY, P. A. 2018. Exploring drivers of litter decomposition in a greening Arctic: results from a transplant experiment across a treeline. *Ecology,* 99**,** 2284-2294.
PEACH, M. & ZEDLER, J. B. 2006. How tussocks structure sedge meadow vegetation. *Wetlands,* 26**,** 322-335.
PENG, C., GUIOT, J., WU, H., JIANG, H. & LUO, Y. 2011. Integrating models with data in ecology and palaeoecology: advances towards a model–data fusion approach. *Ecology Letters,* 14**,** 522-536.
QIAO, X., ZHANG, J., WANG, Z., XU, Y., ZHOU, T., MI, X., CAO, M., YE, W., JIN, G., HAO, Z., WANG, X., WANG, X., TIAN, S., LI, X., XIANG, W., LIU, Y., SHAO, Y., XU, K., SANG, W., ZENG, F., REN, H., JIANG, M. & ELLISON, A. M. 2020. Foundation Species Across a Latitudinal Gradient in China. *Ecology***,** e03234.
R CORE TEAM 2019. R: A language and environment for statistical computing. . Vienna, Austria: R Foundation for Statistical Computing.
RASTETTER, E. B. 2017. Modeling for understanding v. modeling for numbers. *Ecosystems,* 20**,** 215-221.
RICHARDSON, A. D., AUBINET, M., BARR, A. G., HOLLINGER, D. Y., IBROM, A., LASSLOP, G. & REICHSTEIN, M. 2012. Uncertainty quantification. *Eddy covariance.* Springer.
RICHARDSON, A. D., WILLIAMS, M., HOLLINGER, D. Y., MOORE, D. J., DAIL, D. B., DAVIDSON, E. A., SCOTT, N. A., EVANS, R. S., HUGHES, H. & LEE, J. T. 2010. Estimating parameters of a forest ecosystem C model with measurements of stocks and fluxes as joint constraints. *Oecologia,* 164**,** 25-40.
SHAVER, G. R., FETCHER, N. & CHAPIN, F. S. 1986a. Growth and flowering in Eriophorum vaginatum: annual and latitudinal variation. *Ecology,* 67**,** 1524-1535.
SHAVER, G. R., III, F. C. & GARTNER, B. L. 1986b. Factors Limiting Seasonal Growth and Peak Biomass Accumulation in Eriophorum Vaginatum in Alaskan Tussock Tundra. *The Journal of Ecology,* 74.

SOETAERT, K. E., PETZOLDT, T. & SETZER, R. W. 2010. Solving differential equations in R: package deSolve. *Journal of statistical software,* 33.

STEPHENSON, K. 2003. Circle packing: a mathematical tale. *Notices of the AMS,* 50**,** 1376-1388.

STUART, L. & MILLER, P. C. 1982a. Effect of fertilization, altered drainage and vehicle tracks on soil aeration in tussock tundra. *Canadian Journal of Soil Science,* 62**,** 495-502.

STUART, L. & MILLER, P. C. 1982b. Soil oxygen flux measured polarographically in an Alaskan tussock tundra. *Ecography,* 5**,** 139-144.

VARTY, A. K. & ZEDLER, J. B. 2008. How waterlogged microsites help an annual plant persist among salt marsh perennials. *Estuaries and Coasts,* 31**,** 300-312.

WEIN, R. W. 1973. Eriophorum vaginatum L. *Journal of Ecology,* 61**,** 601-615.

WOLFRAM, S. 2002. *A new kind of science*, Wolfram media Champaign, IL.

WRIGHT, K. S. & ROCHA, A. V. 2018. A test of functional convergence in carbon fluxes from coupled C and N cycles in Arctic tundra. *Ecological Modelling,* 383**,** 31-40.

ZOBITZ, J., DESAI, A., MOORE, D. & CHADWICK, M. 2011. A primer for data assimilation with ecological models using Markov Chain Monte Carlo (MCMC). *Oecologia,* 167**,** 599-611.